

A Time Optimal Trajectory Planning Method for Overhead Cranes with Obstacle Avoidance

He Chen¹, Peng Yang^{1†}, and Yanli Geng¹

Abstract—Overhead cranes are commonly seen industrial transportation tools. However, some obstacles may exist on the payload transportation path. To deal with this kind of problem, here, an obstacle avoidance considered trajectory planning algorithm is designed for overhead crane systems. Specifically, to achieve the obstacle avoidance objective, we decide to design trolley moving trajectories and the payload hoisting/lowering trajectories. After carefully analyzing the crane system kinematic model with payload hoisting/lowering, it is found that this system is differentially flat. By using the flatness theory, the planning problem for trolley movements and the payload hoisting/lowering is solved by planning suitable trajectories for the system flat outputs. During the planning process, various system constraints are carefully considered. Additionally, the idea of bisection is used to obtain the optimal transportation time. At last, the proposed method is tested by simulations to verify its satisfactory performance.

I. INTRODUCTION

In industrial production, various cranes [1]–[7] are effective transportation tools. To reduce costs and simplify mechanical structure, the payload of a crane system cannot be directly controlled, which is usually dragged by a trolley or a jib through a steel rope. This kind of structure leads to the act that the control inputs of a crane system are usually less than corresponding degrees of freedom (DOFs), which means that crane systems are typical underactuated systems [8]. Different from full-actuated systems like robot manipulators [9], the underactuated property increases the control difficulty of crane systems and in industry, and most cranes are manipulated manually. However, manual operation usually has disadvantages like lower working efficiency, poor positioning accuracy, etc. To obtain better control performance, automatic control methods are urgently needed.

Among all crane systems, the overhead crane is widely seen. This system has two parts of control objective. The first one is to make the trolley move to the target position quickly and accurately; the second is to suppress the payload swing. However, it is found that high couplings exist between system states, inappropriate trolley acceleration or deceleration movements may cause large payload swing, which should be avoided. Additionally, other properties like dead-zone [10], time-delay, may also increase the control difficulty of crane systems. Recently, this difficult problem

has become one of the research hot spots and scholars all over the world have focused on this problem with lots of methods being presented. To effectively suppress the payload swing, control method by using input shaping are proposed by carefully shaping the trolley actuating force based on the system natural frequency [11]–[13]. By deeply analyzing the crane coupling behavior, carefully designed trolley trajectory can be obtained, by following which, the objective of trolley positioning could be achieved with swing suppression. Based on this idea, [14]–[18] present different kinds of trajectories. For example, in [14], based on a discrete system model, optimal trolley trajectories, known as time-optimal trajectory, swing-optimal trajectory, and energy-optimal trajectory, are respectively planned for the trolley by taking into account various system constraints.

In addition, to obtain better closed-loop system robustness, scholars also designs some closed-loop control methods. [19], [20] give effective method by using passivity property, which are proven to bring asymptotical stability results. Since some physical parameters are difficult to measure, researchers present adaptive-based methods in [21], [22]. Considering the fact that the working situations of overhead cranes are complicated with disturbances, SMC-based methods are also successfully used to control overhead cranes and obtain proper robustness [23], [24]. A model predictive control-based method is proposed in [25], which can deal with the payload swing constraints. Additionally, some intelligence-based control methods, including neural network-based control methods [26], [27], fuzzy logic-based control methods [28], [29], and so forth, are also shown to be effective.

Though the crane control problem has been widely studied, there still exist some to-be-solved problems. In industry, since the working environment of an overhead crane is very complex, some obstacles may exist on the payload transportation path. To avoid possible collisions, the obstacle avoidance objective should be considered. However, there are few methods considering this problem. Based on this fact, here, we are expected to design an optimal trajectory planning method with obstacle avoidance. In particular, the payload hoisting and lowering movements are added in the transportation task to achieve the obstacle avoidance objective. By deeply analyzing the system model, the overhead crane is shown to be differentially flat and the flatness property is used to deal with couplings between system states. By considering various system constraints including swing angle, angular velocity, trolley velocity, and trolley acceleration constraints, we construct an optimization problem

This work is supported in part by the National Natural Science Foundation of China (61803143).

¹He Chen, Peng Yang, and Yanli Geng are with the School of Artificial Intelligence, Hebei University of Technology, Tianjin 300401, China. chenhe@hebut.edu.cn; ypphebut@163.com; gengyl@hebut.edu.cn

[†]To whom correspondence should be addressed.

with respect to time. Utilizing a bisection-based method, the optimization problem is solved with optimal transportation time being obtained. Additionally, some numerical simulations are included to testify our method.

The rest part is shown as follows: In Section II, we give the system dynamic model as well as the detailed control objective. Section III gives the entire trajectory planning process with obstacle avoidance. Section IV illustrates results for simulations. At last, the entire paper is summarised in Section V.

II. PROBLEM STATEMENT

Here, we consider a crane control problem, whose dynamic model is illustrate as follows [21]:

$$(M + m)\ddot{x} + m\ddot{\theta}\cos\theta + m\ddot{l}\sin\theta + 2m\dot{l}\dot{\theta}\cos\theta - m\dot{\theta}^2\sin\theta = F_t, \quad (1)$$

$$m\ddot{l} + m\ddot{x}\sin\theta - m\dot{\theta}^2 - mg\cos\theta = F_l, \quad (2)$$

$$ml^2\ddot{\theta} + ml\cos\theta\ddot{x} + 2ml\dot{\theta}\dot{x} + mgl\sin\theta = 0, \quad (3)$$

where $x(t)$, $\theta(t)$, $l(t)$ denote the trolley movement, the payload swing angle, and the varying rope length, respectively, $F_t(t)$, $F_l(t)$ respectively represent the trolley actuating force and the hoisting/lowering actuating force, m , M are masses of the payload and the trolley, respectively, g is the gravity acceleration constant.

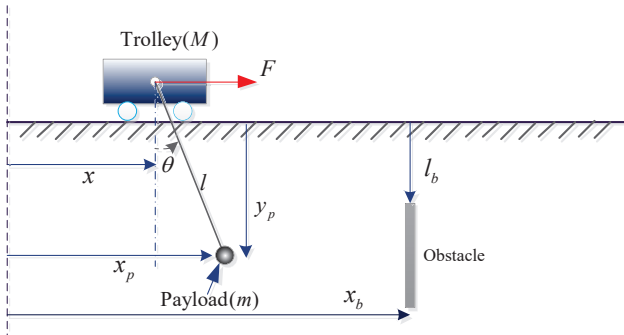


Fig. 1. Illustration of obstacle avoidance.

As we all know, the crane control objective includes two parts, fast and accurate trolley moving and swing elimination, which can be achieved by properly controlling the trolley movement. However, since an overhead crane may be in various situations, there probably exist obstacles on the payload transportation path, as shown in Fig. 1. If the obstacle avoidance is not considered, accidents like collisions may occur, which is very dangerous. Based on this fact, in this paper, we are expected to design a suitable control method with payload hoisting/lowering to achieve the obstacle avoidance. In particular, the crane control objectives with obstacle avoidance are listed as follows:

- Regulate the trolley to its desired position x_d from the initial position x_i .
- Assume that there exists an obstacle at x_b as shown in Fig. 1, and to achieve the obstacle avoidance objective,

the payload should be hoisted to ensure that, when the payload horizontal position $x_p(t)$ reaches x_b , the payload vertical position $y_p(t)$ reaches l_b from its initial value l_i . Additionally, to finish the transportation, when the payload passes x_b , the payload should be lowered, and when the payload reaches its desired position x_d , the payload vertical position $y_p(t)$ should reach its initial value l_i .

- Eliminate the payload swing $\theta(t)$ effectively with the trolley moving.

In the next section, we will give a useful method to achieve the aforementioned control objectives.

III. TRAJECTORY PLANNING

A. Flat Output Construction

We first focus on the kinematic model in (3). By using small-angle assumption¹, (3) is linearized as follows:

$$l\ddot{\theta} + \ddot{x} + 2\dot{l}\dot{\theta} + g\theta = 0. \quad (4)$$

On the other hand, the coordinate of the payload is shown as

$$x_p = x + l\theta, \quad y_p = l, \quad (5)$$

where $x_p(t)$ and $y_p(t)$ respectively denote the horizontal and vertical positions of the payload. Taking the time derivative of (5) twice, then we have

$$\ddot{x}_p = \ddot{x} + \ddot{l}\theta + 2\dot{l}\dot{\theta} + l\ddot{\theta}, \quad \ddot{y}_p = \ddot{l}. \quad (6)$$

Substituting (6) into (4), we can obtain

$$\theta = -\frac{\ddot{x}_p}{g - \ddot{y}_p}. \quad (7)$$

Then, by using (5) and (7), the trolley displacement is described as

$$x = x_p + \frac{y_p\ddot{x}_p}{g - \ddot{y}_p}. \quad (8)$$

From (5), (7), and (8), it is found that all state variables $x(t)$, $l(t)$, $\theta(t)$ can be expressed by using $x_p(t)$ and $y_p(t)$. Therefore, we can conclude that the overhead crane system is differentially flat with the payload coordinates as the flat outputs.

B. Optimization Problem Construction

To calculate the optimal time, we should construct a time optimization problem considering the following conditions:

- 1) To finish the transportation task, the trolley ought to get the destination x_d at time $t = T$ from its initial position x_i at time $t = 0$, while velocity and acceleration signals ought to be zero. In addition, $\theta(t)$ and $\dot{\theta}(t)$ should also be zero at time $t = 0$ and $t = T$. Then we have

$$x(0) = x_i, \dot{x}(0) = 0, \ddot{x}(0) = 0, \quad (9)$$

$$x(T) = x_d, \dot{x}(T) = 0, \ddot{x}(T) = 0, \quad (10)$$

$$\theta(0) = 0, \dot{\theta}(0) = 0, \theta(T) = 0, \dot{\theta}(T) = 0. \quad (11)$$

¹The small-angle approximation is usually established in the transportation [12], [14], which means that $\sin\theta \approx \theta$, $\cos\theta \approx 1$.

- 2) To achieve obstacle avoidance, the payload should be hoisted at first. When the payload horizontal position $x_p(t)$ reaches x_b at time $t = t_s$, the payload vertical position $y_p(t)$ should reach l_b . Then the payload should be lowered to finish the transportation task. When $x_p(t)$ reaches x_d at $t = T$, $y_p(t)$ reaches its initial position l_i . Additionally, the payload vertical velocity and acceleration ought to be zero when $t = 0$, $t = t_s$, and $t = T$. Thus we have the following relationship:

$$y_p(0) = l_i, \dot{y}_p(0) = 0, \ddot{y}_p(0) = 0, \quad (12)$$

$$y_p(t_s) = l_b, \dot{y}_p(t_s) = 0, \ddot{y}_p(t_s) = 0, \quad (13)$$

$$y_p(T) = l_i, \dot{y}_p(T) = 0, \ddot{y}_p(T) = 0, \quad (14)$$

where l_i is the initial value of the payload vertical position which is also the initial rope length.

- 3) In the entire control task, the trolley velocity and acceleration should be kept in suitable ranges. Additionally, the payload swing angle and angular velocity should also be limited in corresponding suitable ranges to ensure safety, in the sense that

$$|\dot{x}(t)| \leq v_{\max}, |\ddot{x}(t)| \leq a_{\max}, \quad (15)$$

$$|\theta(t)| \leq \theta_{\max}, |\dot{\theta}(t)| \leq w_{\max}, \quad (16)$$

wherein v_{\max} , a_{\max} , θ_{\max} , w_{\max} represent the permitted trolley velocity, acceleration, payload swing angle, and angular velocity amplitudes, respectively.

After that, substituting (7) and (8) into (9)–(11), (15), and (16) and doing some calculations, we have the following results:

$$x_p(0) = x_i, \dot{x}_p(0) = 0, \ddot{x}_p(0) = 0, x_p^{(3)}(0) = 0, \quad (17)$$

$$x_p^{(4)}(0) = 0, x_p(T) = x_d, \dot{x}_p(T) = 0, \ddot{x}_p(T) = 0, \quad (18)$$

$$x_p^{(3)}(T) = 0, x_p^{(4)}(T) = 0, \quad (19)$$

$$\left| \frac{\ddot{x}_p}{g - \ddot{y}_p} \right| \leq \theta_{\max}, \left| \frac{x_p^{(3)}(g - \ddot{y}_p) + y_p^{(3)}\ddot{x}_p}{(g - \ddot{y}_p)^2} \right| \leq w_{\max}, \quad (20)$$

$$\left| \dot{x}_p + \frac{\dot{y}_p\ddot{x}_p}{g - \ddot{y}_p} + \frac{y_p[x_p^{(3)}(g - \ddot{y}_p) + y_p^{(3)}\ddot{x}_p]}{(g - \ddot{y}_p)^2} \right| \leq v_{\max}, \quad (21)$$

$$\left| \ddot{x}_p + \frac{\ddot{y}_p\ddot{x}_p}{g - \ddot{y}_p} + \frac{2\dot{y}_p[x_p^{(3)}(g - \ddot{y}_p) + y_p^{(3)}\ddot{x}_p]}{(g - \ddot{y}_p)^2} + \frac{y_p}{(g - \ddot{y}_p)^4} \cdot \left\{ [x_p^{(4)}(g - \ddot{y}_p) + y_p^{(4)}] \cdot (g - \ddot{y}_p)^2 + 2(g - \ddot{y}_p) \cdot y_p^{(3)} \right. \right. \\ \left. \left. \cdot [x_p^{(3)}(g - \ddot{y}_p) + y_p^{(3)}\ddot{x}_p] \right\} \right| \leq a_{\max}. \quad (22)$$

Now it is found that all constraints shown in (12)–(14) and (17)–(22) are with respect to $x_p(t)$ and $y_p(t)$ and we can construct a time optimization problem as

$$\text{minimize} \quad T \quad (23)$$

subject to (12) – (14) and (17) – (22).

Next, we will solve the optimization problem to obtain the optimal trolley displacement and rope length reference trajectories.

C. Optimization Problem Solution

We first analyze the equality constraints with respect to $x_p(t)$ as shown in (17)–(19). It is found that there exist 10 equality constraints and thus we choose a 9-order polynomial function to express $x_p(t)$, which is shown as follows:

$$x_p(t) = (x_d - x_i) \cdot \sum_{i=0}^9 \alpha_i \left(\frac{t}{T}\right)^i + x_i, \quad (24)$$

where α_i 's, $i = \{0, 1, \dots, 9\}$ are to-be-determined parameters. Then the n th-order derivative of $x_p(t)$ is calculated as:

$$x_p^{(n)}(t) = (x_d - x_i) \cdot \sum_{i=n}^9 \alpha_i \frac{i!}{(i-n)!} \left(\frac{1}{T}\right)^n \left(\frac{t}{T}\right)^{i-n}. \quad (25)$$

Substituting (24) and (25) into (17)–(19) and doing some calculations, we can obtain

$$\alpha_0 = \alpha_1 = \alpha_2 = \alpha_3 = \alpha_4 = 0, \quad \alpha_5 = 126,$$

$$\alpha_6 = -420, \quad \alpha_7 = 540, \quad \alpha_8 = -315, \quad \alpha_9 = 70.$$

Next, after carefully analyzing equality constraints with respect to $y_p(t)$ shown in (12)–(14), $y_p(t)$ is constructed by using a 5-order piecewise polynomial function shown as follows:

$$y_p(t) = \begin{cases} (l_b - l_i) \cdot \sum_{i=0}^5 \beta_i \left(\frac{t}{t_s}\right)^i + l_i, & t \in [0, t_s], \\ (l_i - l_b) \cdot \sum_{i=0}^5 \beta_i \left(\frac{t-t_s}{T-t_s}\right)^i + l_b, & t \in [t_s, T], \end{cases} \quad (26)$$

where β_i 's, $i \in \{0, 1, 2, \dots, 5\}$ represent to-be-determined parameters and t_s denotes the time when the payload horizontal position reaches x_b , which can be obtained by solving the equation $x_p(t) = x_b$. Then, based on (26) and (12)–(14), we have

$$\beta_0 = \beta_1 = \beta_2 = 0, \quad \beta_3 = 10, \quad \beta_4 = -15, \quad \beta_5 = 6.$$

Algorithm 1 Detailed processes of solving (23)

Input: $x_i, x_d, x_b, l_i, l_b, \alpha_i, \beta_i, v_{\max}, a_{\max}, \theta_{\max}, w_{\max}, T_1, T_2, \delta$.

Output: T^* .

```

1  while  $T_2 - T_c > \delta$  do
2    set:  $T = (T_1 + T_2)/2$ 
3    if (20)–(22) are all satisfied then
4       $T_2 = T$ 
5    else
6       $T_1 = T$ 
7    end if
8  end while
9   $T^* = T_2$ .
```

To solve the time optimization problem shown in (23) and obtain the optimal transportation time, we use a bisection-based method, whose detailed process of the bisection-based method is shown in **Algorithm 1** by pseudo codes, where

T_1, T_2 respectively represent the lower and upper bounds of T^* , $\delta \in \mathbb{R}^+$ is the permitted optimization error. Utilizing **Algorithm 1**, (23) can be solved with optimal transportation time T^* obtained. Based on (5) and (8), we can construct the reference trajectories for $x(t)$ and $l(t)$ as follows:

$$x_r = \begin{cases} x_p + \frac{y_p \ddot{x}_p}{g - \ddot{y}_p}, & t \in [0, T^*], \\ x_d, & t > T^* \end{cases}, \quad (27)$$

$$l_r = \begin{cases} y_p, & t \in [0, T^*], \\ l_i, & t > T^* \end{cases}. \quad (28)$$

Now, the entire trajectory planning process with obstacle avoidance is finished.

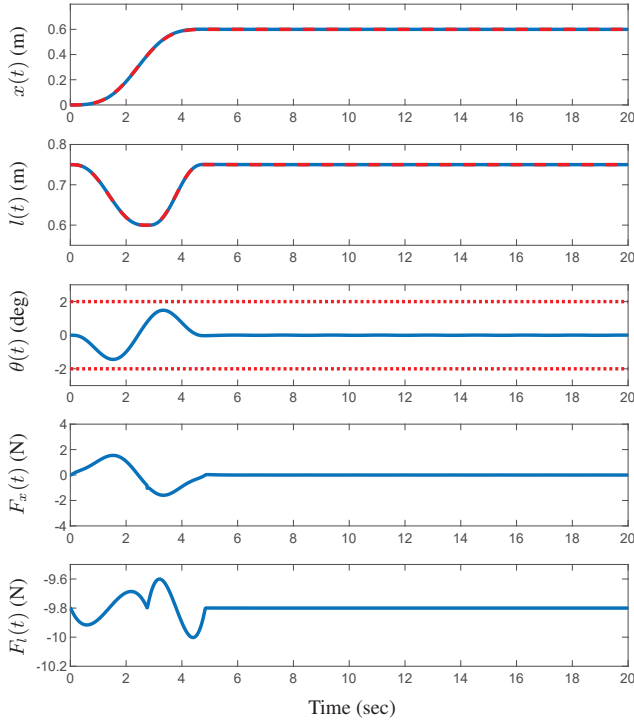


Fig. 2. Simulation results (the trolley displacement, the rope length, the swing angle, the trolley actuating force, and the hoisting/lowering force). Blue solid line: simulation results; red dashed line: reference trajectories $x_r(t)$, $l_r(t)$; red dotted line: swing angle constraint $\theta_{\max} = 2$ deg.

IV. SIMULATION RESULTS

To test the designed method, we give some simulations by using MATLAB/Simulink. The used parameters are set as

$$M = 6.5 \text{ kg}, m = 1 \text{ kg}, x_i = 0 \text{ m}, x_d = 0.6 \text{ m}, \\ x_b = 0.4 \text{ m}, g = 9.8 \text{ m/s}^2, l_i = 0.75 \text{ m}, l_b = 0.6 \text{ m}.$$

The permitted amplitudes are selected as

$$v_{\max} = 0.4 \text{ m/s}, a_{\max} = 0.2 \text{ m/s}^2, \\ \theta_{\max} = 2 \text{ deg}, w_{\max} = 3 \text{ deg/s}.$$

For the bisection method shown in **Algorithm 1**, the parameters are set as

$$T_1 = 0 \text{ s}, T_2 = 20 \text{ s}, \delta = 0.0001.$$

By utilizing MATLAB, the optimization problem is solved with the optimal time as $T^* = 4.8299$ s. Then to finish the trajectory tracking process, the proportional differential (PD) control method is used with the following expressions:

$$F_t = -k_{p1}(x - x_r) - k_{d1}(\dot{x} - \dot{x}_r), \\ F_l = -k_{p2}(l - l_r) - k_{d2}(\dot{l} - \dot{l}_r) - mg \cos \theta,$$

where $k_{p1}, k_{d1}, k_{p2}, k_{d2} \in \mathbb{R}^+$ are positive control gains, which are selected as follows after carefully tuning:

$$k_{p1} = 500, k_{d1} = 200, k_{p2} = 100, k_{d2} = 100.$$

The simulation results are shown in Figs. 2–4. In these figures, it is found that using the designed method, the trolley can reach the desired position fast and accurately within the optimal transportation time T^* . In addition, from Fig. 4, we can see that when $x_p(t)$ reaches x_b , the payload vertical position $y_p(t)$ reaches l_b , which means that the obstacle avoidance objective is successfully achieved. Beyond that, the swing angle is effectively eliminated with no residual

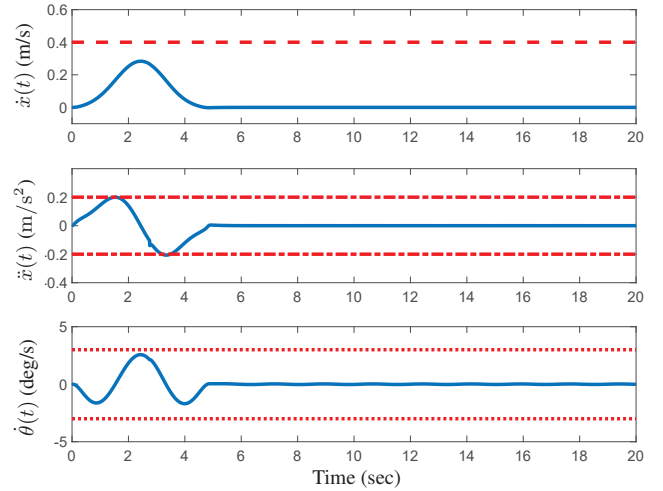


Fig. 3. Simulation results (the trolley velocity, the trolley acceleration, and the angular velocity). Blue solid line: simulation results; red dashed line: trolley velocity range $v_{\max} = 0.4$ m/s; red dotted-dashed line: trolley acceleration range $a_{\max} = 0.2$ m/s²; red dotted line: angular velocity range $w_{\max} = 3$ deg/s.

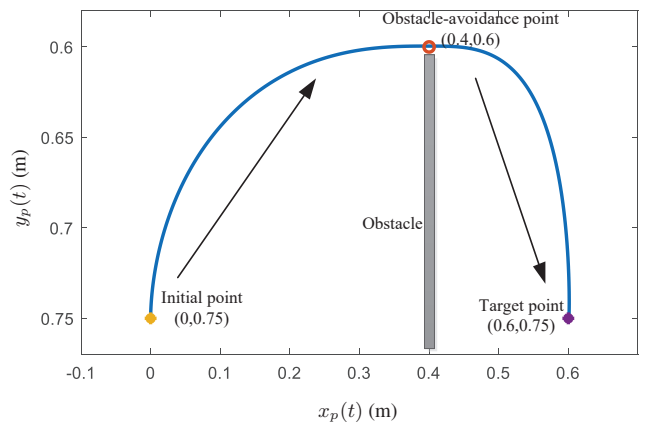


Fig. 4. Simulation results (the payload position).

swing after the transportation. Additionally, the trolley velocity, trolley acceleration, swing angle, swing angular velocity constraints are all ensured. In summary, it is concluded that the trajectory planning method achieves the objectives of overhead crane systems with obstacle avoidance.

V. CONCLUSION

Considering the obstacle avoidance objective, we propose an obstacle avoidance considered trajectory planning method, which achieves fast and proper trolley positioning and payload swing suppression, together with obstacle avoidance. Specifically, to achieve the obstacle avoidance objective, we decide to add payload hoisting and lowering movements in the transportation task. By carefully analyzing the kinematic model, the overhead crane is shown to be differentially flat with the payload horizontal and vertical positions as the flat outputs. Then the original trajectory planning is converted into the trajectory planning for flat outputs. By taking into account various constraints, a time optimization problem is formulated. Utilizing a bisection-based method, the optimization problem is solved with the optimal transportation time, as well as optimal reference trajectories, being obtained. At last, some simulations are given to test the design method.

REFERENCES

- [1] J. Smoczek and J. Szpytko, "Particle swarm optimization-based multivariable generalized predictive control for an overhead crane," *IEEE/ASME Transactions on Mechatronics*, vol. 22, no. 1, pp. 258–268, 2017.
- [2] N. Sun, Y. Wu, H. Chen, and Y. Fang, "Antiswing cargo transportation of underactuated tower crane systems by a nonlinear controller embedded with an integral term," *IEEE Transactions on Automation Science and Engineering*, in press, DOI: 10.1109/TASE.2018.2889434.
- [3] N. Sun, T. Yang, Y. Fang, Y. Wu, and H. Chen, "Transportation control of double-pendulum cranes with a nonlinear quasi-PID scheme: Design and experiments," *IEEE Transactions on Systems, Man, and Cybernetics: Systems*, in press, DOI: 10.1109/TSMC.2018.2871627.
- [4] H. Chen, Y. Fang, and N. Sun, "An adaptive tracking control method with swing suppression for 4-DOF tower crane systems," *Mechanical Systems and Signal Processing*, vol. 123, pp. 426–442, 2019.
- [5] H. Ouyang, G. Zhang, L. Mei, X. Deng, and D. Wang, "Load vibration reduction in rotary cranes using robust two-degree-of-freedom control approach," *Advances in Mechanical Engineering*, vol. 8, no. 3, pp. 1–11, 2016.
- [6] N. Sun, T. Yang, H. Chen, Y. Fang, and Y. Qian, "Adaptive anti-swing and positioning control for 4-DOF rotary cranes subject to uncertain/unknown parameters with hardware experiments," *IEEE Transactions on Systems, Man, and Cybernetics: Systems*, in press, DOI: 10.1109/TSMC.2017.2765183.
- [7] N. Sun, Y. Fang, H. Chen, Y. Fu, and B. Lu, "Nonlinear stabilizing control for ship-mounted cranes with ship roll and heave movements: Design, analysis, and experiments," *IEEE Transactions on Systems, Man, and Cybernetics: Systems*, vol. 48, no. 10, pp. 1781–1793, 2018.
- [8] J. G. Romero, A. Donaire, R. Ortega, and P. Borja, "Global stabilization of underactuated mechanical systems via PID passivity-based control," *Automatica*, vol. 96, pp. 178–185, 2018.
- [9] Q. Zhou, S. Zhao, H. Li, R. Lu and, C. Wu, "Adaptive neural network tracking control for robotic manipulators with dead-zone," *IEEE Transactions on Neural Networks and Learning Systems*, DOI: 10.1109/TNNLS.2018.286937.
- [10] H. Li, S. Zhao, W. He and, R. Lu, "Adaptive finite-time tracking control of full states constrained nonlinear systems with dead-zone," *Automatica*, vol. 100, pp. 99–107, 2019.
- [11] L. Ramli, Z. Mohamed, and H. I. Jaafar, "A neural network-based input shaping for swing suppression of an overhead crane under payload hoisting and mass variations," *Mechanical Systems and Signal Processing*, vol. 107, pp. 484–501, 2018.
- [12] D. Blackburn, W. Singhose, J. Kitchen, V. Patrangenaru, J. Lawrence, T. Kamoi, and A. Taura, "Command shaping for nonlinear crane dynamics," *Journal of Vibration and Control*, vol. 16, no. 4, pp. 477–501, 2010.
- [13] M. J. Maghsoudi, Z. Mohamed, M.O. Tokhi, A.R. Husain, and M.S.Z. Abidin, "Control of a gantry crane using input-shaping schemes with distributed delay," *Transactions of the Institute of Measurement and Control*, vol. 39, no. 3, pp. 361–370, 2017.
- [14] Z. Wu and X. Xia, "Optimal motion planning for overhead cranes," *IET Control Theory & Applications*, vol. 8, no. 17, pp. 1833–1842, 2014.
- [15] H. Rams, M. Schöberl, and K. Schlacher, "Optimal motion planning and energy-based control of a single mast stacker crane," *IEEE Transactions on Control Systems Technology*, vol. 26, no. 4, pp. 1449–1457, 2018.
- [16] N. Sun, Y. Wu, H. Chen, and Y. Fang, "An energy-optimal solution for transportation control of cranes with double pendulum dynamics: Design and experiments," *Mechanical Systems and Signal Processing*, vol. 102, pp. 87–101, 2018.
- [17] H.-H. Lee, "Motion planning for three-dimensional overhead cranes with high-speed load hoisting," *International Journal of Control*, vol. 78, no. 12, pp. 875–886, 2005.
- [18] H. Chen, Y. Fang, and N. Sun, "A swing constrained time-optimal trajectory planning strategy for double pendulum crane systems," *Nonlinear Dynamics*, Vol. 89, no. 2, pp. 1513–1524, 2017.
- [19] X. Wu and X. He, "Nonlinear energy-based regulation control of three-dimensional overhead cranes," *IEEE Transactions on Automation Science and Engineering*, vol. 14, no. 2, pp. 1297–1308, 2017.
- [20] N. Sun, Y. Fang, and X. Zhang, "Energy coupling output feedback control of 4-DOF underactuated cranes with saturated inputs," *Automatica*, vol. 49, no. 5, pp. 1318–1325, 2013.
- [21] N. Sun, Y. Fang, H. Chen, and B. He, "Adaptive nonlinear crane control with load hoisting/lowering and unknown parameters: design and experiments," *IEEE/ASME Transactions on Mechatronics*, vol. 20, no. 5, pp. 2107–2119, 2015.
- [22] Z. Zhang, Y. Wu, and J. Huang, "Robust adaptive antiswing control of underactuated crane systems with two parallel payloads and rail length constraint," *ISA Transactions*, vol. 65, pp. 275–283, 2016.
- [23] M.-S. Park, D. Chwa, and M. Eom, "Adaptive sliding-mode antisway control of uncertain overhead cranes with high-speed hoisting motion," *IEEE Transactions on Fuzzy Systems*, vol. 22, no. 5, pp. 1262–1271, 2014.
- [24] D. Chwa, "Sliding-mode-control-based robust finite-time antisway tracking control of 3-D overhead cranes," *IEEE Transactions on Industrial Electronics*, vol. 64, no. 8, pp. 6775–6784, 2017.
- [25] H. Chen, Y. Fang, and N. Sun, "A swing constraint guaranteed MPC algorithm for underactuated overhead cranes," *IEEE/ASME Transactions on Mechatronics*, vol. 21, no. 5, pp. 2543–2555, 2016.
- [26] D. Wang, H. He, and D. Liu, "Intelligent optimal control with critic learning for a nonlinear overhead crane system," *IEEE Transactions on Industrial Informatics*, vol. 14, no. 7, pp. 2932–2940, 2018.
- [27] T. Yang, N. Sun, H. Chen, and Y. Fang, "Neural network-based adaptive antiswing control of an underactuated ship-mounted crane with roll motions and input dead-zones," *IEEE Transactions on Neural Networks and Learning Systems*, in press, DOI: 10.1109/TNNLS.2019.2910580.
- [28] Z. Sun, Y. Bi, X. Zhao, Z. Sun, C. Ying, and S. Tan, "Type-2 fuzzy sliding mode anti-swing controller design and optimization for overhead crane," *IEEE Access*, vol. 6, pp. 51931–51938, 2018.
- [29] H. Chen, Y. Fang, and N. Sun, "A payload swing suppression guaranteed emergency braking method for overhead crane systems," *Journal of Vibration and Control*, vol. 24, no. 20, pp. 4651–4660, 2018.